Forward and inverse kinematic analyses of a developed and evaluated bricklaying gantry-based parallel robot manipulator

Musa Hassan Ibrahim[1], Umar Ali Umar[1, *], Matthew Afolayan Olatunde[1]

[1]Department of Mechanical Engineering, Ahmadu Bello University, Zaria, 810107, Nigeria

[*]Corresponding Author: Umar Ali Umar. Email: umaraliumar@yahoo.co.uk

Abstract: Gantry robots are still used in wide application areas, especially pick and place applications. However, their kinematic modeling is associated with transforming positions and velocitiesin several base frames to each other. Generally, there are two types of kinematics as regards position, forward (direct) kinematics and inverse kinematics. Forward kinematics deals with determing the position (spot/location) and orientation of the end-effector while given the joint variables. Thus, the inverse kinematics is associated with finding the joint variables while given the position and orientation of the end-effector. Hence, this research presents a study in the field of forward and inverse kinematics modeling on the aforementioned robot through an attempt to provide a better solution enhancing kinematics simplicity. In this study, mathematical functions and equations were used, including the likes of algebra, trigonometry, geometry and a knowledge of motion mechanics was also applied. This study used a two-method kinematic analysis procedure for the forward kinematics. The results shows a range of values for the displacements and orientation of the links. Two experimental procedures gave a maximum difference of 0.03rad/s and 0.47rad using the first setup and 0.001rad/s and 0.016rad using the second setup, in the displacement and orientation of the links respectively. The inverse kinematics gave a displacent result of A(5mm), B(8.61mm), and C(7mm) and orientation of $A'(71.53^0)$, $B(90.11^0)$ and $C'(125.61^0)$.

Keywords: Gantry robot, Kinematic modeling, Forward and Inverse kinematics, Mathematical functions and equations, Displacement, Orientation.

التحليلات الحركية الأمامية والعكسية للروبوت المتوازي المبني على جسر الرافعة المطور والمقيم

الملخص: لا تزال الروبوتات العملاقة تستخدم في مجالات التطبيقات الواسعة، وخاصة تطبيقات الالتقاط والوضع. ومع ذلك، فإن النمذجة الحركية الخاصة بهم ترتبط بتحويل المواضع والسرعات في العديد من الإطارات الأساسية لبعضها البعض. بشكل عام، هناك نوعان من الكينماتيكا فيما يتعلق بالموضع، الكينماتيكا الأمامية (المباشرة) والحركية العكسية. تتعامل الكينماتيكا الأمامية مع تحديد الموضع (المكان/الموقع) واتجاه المؤثر النهائي مع إعطاء المتغيرات المشتركة. وبالتالي، ترتبط الكينماتيكا العكسية بإيجاد المتغيرات المشتركة مع إعطاء موضع واتجاه المؤثر النهائي. ومن هنا يقدم هذا البحث دراسة في مجال النمذجة الحركية الأمامية والعكسية للروبوت المذكور من خلال محاولة تقديم حل أفضل يعزز البساطة الحركية. تم في هذه الدراسة استخدام الدوال والمعادلات الرياضية، بما في ذلك الجبر وعلم المثلثات والهندسة ومعرفة ميكانيكا الحركة. استخدمت هذه الدراسة أسلوبين للتحليل الحركي للحركيات الأمامية. تظهر النتائج نطاقًا من القيم للإزاحات واتجاه الروابط. أعطى إجراءان تجريبيان أقصى فرق قدره 0.03 rad/s و0.47 rad باستخدام الإعداد الأول و0.001 rad/s و0.016 rad باستخدام الإعداد الثاني، في إزاحة واتجاه الوصلات على التوالي. أعطت الكينماتيكا العكسية نتيجة إزاحة A(5mm) ، B(8.61mm)، و C(7mm) واتجاه $A'(71.53^0)$, $B(90.11^0)$ و $C'(125.61^0)$.

1. Introduction

Kinematic modelling is associated with transforming positions and velocities in several base frames to each other. As regards position kinematics, one is associated with two problems to deal with, forward (direct) kinematics and inverse kinematics. The tendency with direct kinematics can be declared as [27]: Given the joint variables, determines the position (spot) and orientation of the end-effector. This implies that the forward or direct kinematics is fundamentally a transformation from base frames in each joint to the Cartesian, room fixed, frame. The inverse kinematics means the inverse transformation, i.e. finding the joint variables from a given spot (position) and orientation of the end-effector.

The forward kinematics transformation is stated in equation1

$$\begin{pmatrix} x \\ r \end{pmatrix} = f(q) \quad \text{---------- (1)}$$

Where $x \in R^3$ is the location of the end-effector in the Cartesian plane and r portrays or be writes the orientation of the end-effector.

This shows that for a serial kinematic manipulator, the forward kinematics can be derived relatively easily. Beginning from the bottom of the robot, determination of the position and orientation of any joint in the kinematic chain from the joint variables can be achieved by making use of the rotations and displacements in the same order as the joints. This shows fundamentally how the problem is resolved. Generally, inverse kinematics is the most difficult problem and often gives more than just one solution, relying on the DOF of the robot in observation. In order to make the calculations of the kinematic relationships more thorough, one can usually make use of the Denavit-Hartenberg representation [28], [27].

The problem of relating the linear and the angular velocities of the end-effector with the joint velocities is known as velocity kinematics. The manipulator Jacobian, as defined below, is regarded one of the most important quantities in the analysis of robot motion, when deriving these relationships. Beginning with the forward kinematics, a collection of equations that transforms the positions of joint to end-effector position (location) and orientation are given. The Jacobian gives the relationships between the velocities, see equation 2.

$$\begin{pmatrix} \dot{x} \\ \dot{r} \end{pmatrix} = \begin{pmatrix} v \\ w \end{pmatrix} = J(q)\dot{q} \quad \text{---------- (2)}$$

The Jacobian is simply a matrix-valued function enclosing the partial derivatives of the position kinematic relationships. The Jacobian shows up not only here, but also in problems like trajectory planning, determination of singular configurations and derivation of dynamical equations [27]. The inverse velocity kinematics is actually given by the inverse Jacobian (equation 2), supposing that the inverse exists.

The motion analysis of robot manipulators are known as kinematics and kinetics [29]. As regards analysis of kinematics, the position, velocity and acceleration of all the chains are calculated without considering the forces causing the motion. But in robot dynamics, the associated relationship between motions, forces and torques is studied. Screw theory is one of the regarded most active areas in robot kinematics. The aspect of redundancy, avoidance of collision and singularity avoidance is dealt with by robot kinematics. Dealing with kinematics used in the robot, we deal with each of the robot part by assigning a frame of reference to it, hence, a robot with many parts may have many individual frames assigned to each mobile part [30]. For simplicity, single arm of the robot manipulator is dealt with at a time. Each frame is named with numbers systematically, for example, the immobile base of the manipulator is numbered 0, the first link joint to the base is numbered 1, and the next link 2, similarly till the last nth link [31].

Robot kinematics usually are of two types: **forward kinematics** and **inverse kinematics**. Forward kinematics is also called direct kinematics. In forward/direct kinematics, the length of each link and the angle of each joint is given, we therefore calculate the position of all points in the work space of the robot. Where as in inverse/backward kinematics, the length of each link and position of the point in the work volume is given so as to calculate the joint angle [32].

Robot kinematics is grouped into serial manipulator kinematics (SMK), parallel manipulator kinematics (PMK), mobile robot kinematics (MRK) and humanoid kinematics (HK).

The aim of this study is to provide the kinematic analysis of an already developed and evaluated novel gantry-based parallel robot manipulator. Precisely, the research objectives includes the provision of forward and inverse kinematic analysis of the developed and evaluated novel gantry-based parallel robot through the use of mathematical functions and equations, and also by the application of mechanics knowledge. The goal of this study was built on the review of literature as a way to consider the kinematics of gantry robots, particularly forward and inverse kinematics. The review of previous studies on robot manipulators included the study of Afolayan *et al*.[9], who developed a biomorphic carbon-filled natural rubber hyper-redundant joint mechanism robot. The researcher modelled a fish of *teleost* species (a 394.1cm Mackerel) using the biomorphic hyper-redundant joint developed. The study's control algorithm uses built-in motion patterns and the path planning algorithm is sensor-based and both were hosted within a single PIC18F4520 microcontroller. Furthermore, three Futaba 3003 servo motors were used to drive the joints under the control of the microcontroller control algorithm.

Additionally, Karam et al. [10] presented a study on the design, implementation and automation of a multi-robotic processing station. Two robot manipulators, a serial robot manipulator and a parallel robot manipulator of multi-degree of freedom were presented. The design was to develop and test an integrated PRM and SRM system for capping plastic bottles in a scale processing line. Panda *et.al.* [11] developed a gantry material handling robot for use in the bottling industry in food plants. The design was to replace manual labor with an automated system to increase the accuracy, safety and production rate of these plants.

The design was also analyzed from various angles like material selection, cost and simplest and best selection of configuration. Also, Gunnar [12] developed the dynamical analysis and system identification of a Gantry-Tau parallel robot manipulator. The design was to determine the maximum stiffness of the Gantry robot manipulator. The study intended to determine the maximum in the z-direction which was accomplished at the end of the research.

Also, Toby [13], proposed a method called robotic gantry with an end-effector for product lifting. The researcher developed a method that permits the selection of varying portions of a stack of products with the end-effector and protects the selected portions of products using a movable floor. Ye *et al.* [14] developed a variable-scale modular 3D printing robot for building interior walls. The design was to improve the efficiency of construction. The modular robot consisted of a mobile lifting module and a beam printing module. The robot can achieve full printing of complex curved interior walls under different working conditions. Alkali [26] presented a work "design, implementation and automation of a multi-robotic processing station". Two robot manipulators, a serial robot manipulator and parallel robot manipulator of multi degree of freedom were presented.

From the review of literature, it was observed that for most of the robots developed, kinematic analysis was usually missing or not given in details. However, this work thus considers a solution to the gap of kinematic analysis missed for most of the already developed robots. Furthermore, this study can also be applied to kinematically analyze previous studies like that of Gunnar [12] who considered dynamical analysis and system identification of a gantry-tau parallel manipulator, and the study of Panda *et al.* [11] who considered a gantry material handling robot for use in the bottling industry.

2. Materials and methods

2.1 Operation Principle and Control Algorithm of the Gantry Robot

The structure of the robot (figure 1) is a four-frame figured device with dimensions of 550 x 450 x 300 mm. Each leg of the robot mobile platform is considered a serial kinematic chain (KC) made of four-link joints. The y-axis mobile platform is linked to the body frame through a sliding rail situated under, the mobile platform is driven to and fro along the y-axis by a stepper motor mounted under at both sides of the y-axis. The x-axis mobile platform is directly linked to the y-axis with the help of 2 rails placed at the 2 opposite sides of the y-axis, the platform slides forward and backwards horizontally along the 2 rails. The gripper is connected to the x-axis mobile platform and also is manipulated via the aid of the manipulator guide. The end-effector guide ascends and descends along the x-axis mobile platform with the help of a toothed sprocket and chain. The chain is driven by the toothed sprocket, which in turn is driven by a stepper motor situated at the 2 adjacent sides of the x-axis mobile platform. The whole structure is movable on four wheels of 85 mm diameter located at the lower end of the four legs.

The robotic system is made up of three degrees of freedom (ie. 3-DOF).

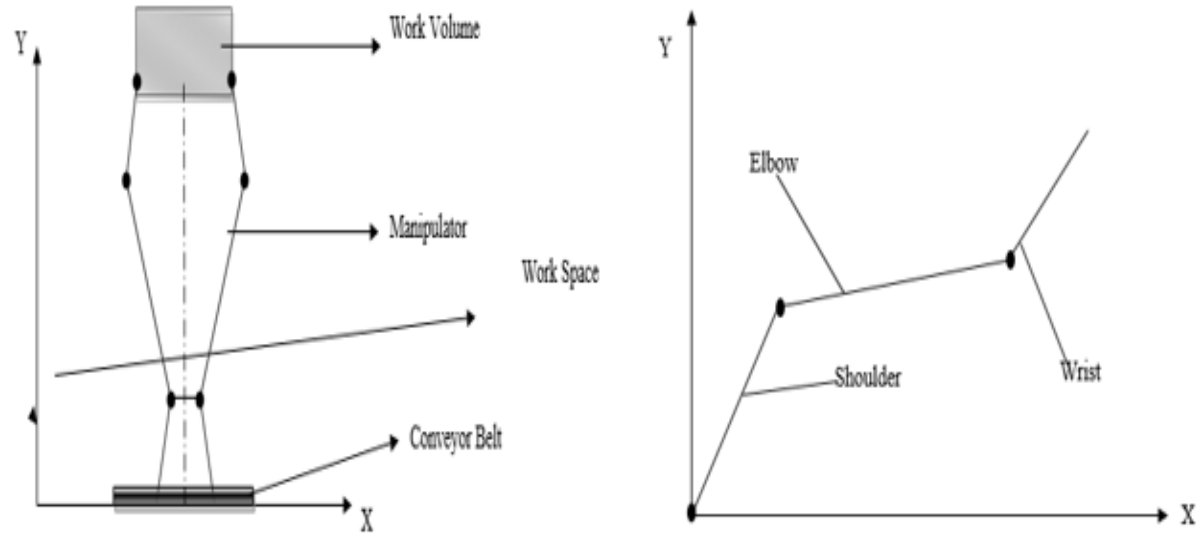

Figure 1: Gantry–based parallel robot manipulator

The control algorithm or operational user guide is shown in Figure 2 as a flowchart. It consists of the procedure of switching on the device, feeding design data, defining the pick/drop spot, and go the next working area when the current design segment is done.

The number of DOF of a robot is the number of independent parameters that must be specified for determining the position of the link relative to the body frame [17]. According to Grubler's criterion and Euler's equation, the DOF of a structure or mechanism/device can be obtained from Equations (1) and (2) [18].

$$m = \lambda(n - j - 1) + \sum_{i=1}^{j} f_i \quad (1)$$

$$L = j - n + 1 \quad (2)$$

For the considered parallel manipulator, $\lambda = 6$, $n = 14$, $j = 15$ and $f_i = 15$, therefore, m=3 (i.e. for motion along x, y & z coordinates).

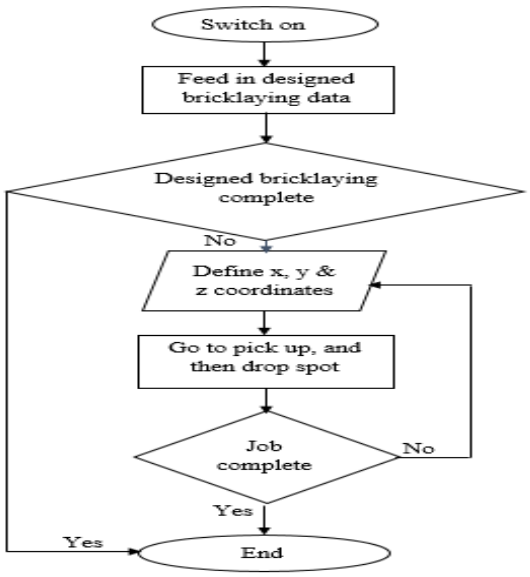

Figure 2: Flow chart showing the algorithm of the Gantry robot

2.2 Forward Kinematic Analysis of the Gantry Robot

"Robot kinematics is mainly of two types: forward and inverse kinematics. Two coordinates are useful for describing the configuration of the system. When attention is focused on the task and end effector, it is preferable to use Cartesian coordinates or end effector coordinates. The other coordinates is called joint coordinates that is useful for describing the configuration of the mechanical linkage. In robotics, it is mandatory to be able to "map" joint coordinates to end effector coordinates. This procedure is refered to as direct kinematics. The procedure that is used to compute joint coordinates for a given end effector coordinates is called inverse kinematics. Basically, this procedure involves solving a set of equations and in general, the equations are nonlinear and complex" [34].

Considering that the robot operates in an x, y plane and the analysis was carried out thus:

Figure 3 shows the plane where the analysis was carried out thus:

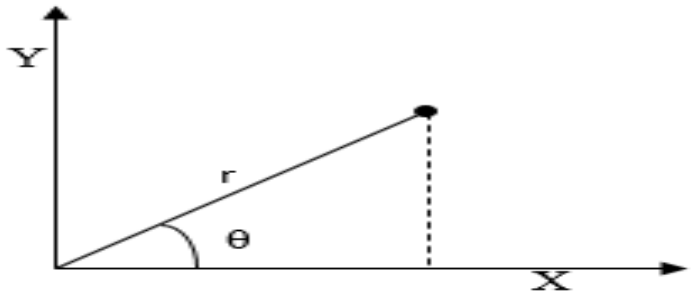

Figure 0: Work space plane of the robot

Where, x = displacement on x-axis in inch, y = displacement on y-axis in inch, r = length of link from the origin (0, 0), that is pick spot to the pre-defined drop spot in inch, θ = angle the link made with the x-axis in degrees, ω = angular velocity in rad/s, and t = 20s (time taken in seconds to pick and drop the block from pick up spot to drop spot)

$$x = r\cos\theta \tag{0}$$

$$y = r\sin\theta \tag{4}$$

$$\theta = \tan^{-1}\left(\frac{y}{x}\right) \tag{5}$$

$$\theta = \omega t \tag{6}$$

From table 1 (first method of experimental approach (1st set up));

Table 1: keeping y-value on level 5 (1st setup)

x (inch)	y (inch)
1.09	4.97
2.04	5.02
2.99	5.01
4.03	4.98
5.13	5.04

When, x = 1.09inch, and y = 4.97inch

$\theta = \tan^{-1}\left(\frac{y}{x}\right)$, (applying equation 5)

» $\theta = \tan^{-1}\left(\frac{4.97}{1.09}\right)$

$\theta = 78^{o}$ (θ = 1.36 rad)

$r = \left(\frac{x}{\cos\theta}\right)$, (applying equation 3)

» $r = \left(\frac{1.09}{\cos 78}\right)$ = 5.24inch, (or, $r = \left(\frac{y}{\sin\theta}\right)$, equation 4)

θ = ωt, (equation 6)

» $\omega = \left(\frac{\theta}{t}\right) = \left(\frac{1.36}{20}\right)$ = 0.070 rad/s

When, x = 2.04inch, and y = 5.02inch

$\theta = tan^{-1}\left(\frac{y}{x}\right)$, (applying equation 5)

» $\theta = tan^{-1}\left(\frac{45.02}{2.04}\right)$

$\theta = 68^{o}$ (θ = 1.19 rad)

$r = \left(\frac{y}{\sin\theta}\right)$, (using equation 4)

» $r = \left(\frac{5.02}{\sin 68}\right)$ = 5.41inch, (or, $r = \left(\frac{x}{\cos\theta}\right)$, equation 3)

θ = ωt, (equation 6)

» $\omega = \left(\frac{\theta}{t}\right) = \left(\frac{1.19}{20}\right)$ = 0.060 rad/s

When, x = 2.99inch, and y = 5.01inch

$\theta = tan^{-1}\left(\frac{y}{x}\right)$, (using equation 5)

» $\theta = tan^{-1}\left(\frac{5.01}{2.99}\right)$

$\theta = 59^{o}$ (θ = 1.03 rad)

$r = \left(\frac{x}{\cos\theta}\right)$, (using equation 3)

» $r = \left(\frac{2.99}{\cos 59}\right)$ = 5.81inch, (or, $r = \left(\frac{y}{\sin\theta}\right)$, equation 4)

θ = ωt, (applying equation 6)

» $\omega = \left(\frac{\theta}{t}\right) = \left(\frac{1.03}{20}\right)$ = 0.052 rad/s

When, x = 4.03inch, and y = 4.98inch

$\theta = tan^{-1}\left(\frac{y}{x}\right)$, (applying equation 5)

» $\theta = tan^{-1}\left(\frac{4.98}{4.03}\right)$

$\theta = 51^{o}$ (θ = 0.890 rad)

$r = \left(\frac{y}{\sin\theta}\right)$, (using equation 4)

» $r = \left(\frac{4.98}{\sin 51}\right)$ = 6.41inch, (or, $r = \left(\frac{x}{\cos\theta}\right)$, equation 3)

θ = ωt, (using equation 6)

» $\omega = \left(\frac{\theta}{t}\right) = \left(\frac{0.890}{20}\right)$ = 0.045 rad/s

When, x = 5.13inch, and y = 5.04inch

$\theta = tan^{-1}\left(\frac{y}{x}\right)$, (applying equation 5)

» $\theta = tan^{-1}\left(\frac{5.04}{5.13}\right)$

$\theta = 45^{o}$ (θ = 0.79 rad)

$r = \left(\frac{x}{\cos\theta}\right)$, (applying equation 3)

» $r = \left(\frac{5.13}{\cos 45}\right)$ = 7.26inch, (or, $r = \left(\frac{y}{\sin\theta}\right)$, equation 4)

θ = ωt, (using equation 6)

» $\omega = \left(\frac{\theta}{t}\right) = \left(\frac{0.79}{20}\right)$ = 0.040 rad/s

From table 2 (second method of experimental approach (2nd set up));

Table 2: Increasing both x & y level values (2nd setup)

x (inch)	y (inch)
1.01	1.04
1.99	2.03
3.01	3.02
3.97	4.01
5.01	5.06

When, x = 1.01inch, and y = 1.04inch

$\theta = tan^{-1}\left(\frac{y}{x}\right)$, (applying equation 5)

» $\theta = tan^{-1}\left(\frac{1.04}{1.01}\right)$

$\theta = 46^{o}$ (θ = 0.803 rad)

$r = \left(\frac{x}{\cos\theta}\right)$, (using equation 3)

» $r = \left(\frac{1.01}{\cos 46}\right)$ = 1.45inch, (or, $r = \left(\frac{y}{\sin\theta}\right)$, equation 4)

θ = ωt, (applying equation 6)

» $\omega = \left(\frac{\theta}{t}\right) = \left(\frac{0.803}{20}\right)$ = 0.040 rad/s

When, x = 1.99inch, and y = 2.03inch

$\theta = tan^{-1}\left(\frac{y}{x}\right)$, (applying equation 5)

» $\theta = tan^{-1}\left(\frac{2.03}{1.99}\right)$

$\theta = 46^o$ (θ = 0.803 rad)

$r = \left(\frac{y}{\sin\theta}\right)$, (using equation 4)

» $r = \left(\frac{2.03}{\sin 46}\right)$ = 2.82inch, (or, $r = \left(\frac{x}{\cos\theta}\right)$, equation 3)

θ = ωt, (applying equation 6)

» $\omega = \left(\frac{\theta}{t}\right) = \left(\frac{0.803}{20}\right)$ = 0.040 rad/s

When, x = 3.01inch, and y = 3.02inch

$\theta = tan^{-1}\left(\frac{y}{x}\right)$, (applying equation 5)

» $\theta = tan^{-1}\left(\frac{1.04}{1.01}\right)$

$\theta = 45.1^o$ (θ = 0.787 rad)

$r = \left(\frac{x}{\cos\theta}\right)$, (using equation 3)

» $r = \left(\frac{3.01}{\cos 45.1}\right)$ = 4.26inch, (or, $r = \left(\frac{y}{\sin\theta}\right)$, equation 4)

θ = ωt, (applying equation 6)

» $\omega = \left(\frac{\theta}{t}\right) = \left(\frac{0.787}{20}\right)$ = 0.039 rad/s

When, x = 3.97inch, and y = 4.01inch

$\theta = tan^{-1}\left(\frac{y}{x}\right)$, (using equation 5)

» $\theta = tan^{-1}\left(\frac{4.01}{3.97}\right)$

$\theta = 45.3^o$ (θ = 0.791 rad)

$r = \left(\frac{y}{\sin\theta}\right)$, (applying equation 4)

» $r = \left(\frac{4.01}{\sin 45.3}\right)$ = 5.64inch, (or, $r = \left(\frac{x}{\cos\theta}\right)$, equation 3)

θ = ωt, (using equation 6)

» $\omega = \left(\frac{\theta}{t}\right) = \left(\frac{0.791}{20}\right)$ = 0.040 rad/s

When, x = 5.01inch, and y = 5.06inch

$\theta = tan^{-1}\left(\frac{y}{x}\right)$, (applying equation 5)

» $\theta = tan^{-1}\left(\frac{5.06}{5.01}\right)$

$\theta = 45.3^{o}$ (θ = 0.791 rad)

$r = \left(\frac{x}{\cos\theta}\right)$, (using equation 3)

» $r = \left(\frac{5.01}{\cos 45.3}\right)$ = 7.12inch, (or, $r = \left(\frac{y}{\sin\theta}\right)$, equation 4)

θ = ωt, (applying equation 6)

» $\omega = \left(\frac{\theta}{t}\right) = \left(\frac{0.791}{20}\right)$ = 0.040 rad/s

2.3 Inverse Kinematic Analysis of the Gantry Robot

i. For a Gantry robot: - The motion design (target motion) and the stepper motor motions are linearly related.

Note: The gantry robot manipulator constitutes a number of links in x, y & z plane axes. The combination of those links forms a kinematic chain (from base to end-effect). Thus, for simplicity possibility of the robot kinematic analysis, it was assumed that this kinematic chain forms a serial arm having shoulder, elbow, and wrist in terms of x, y, z axes.

Thus, for the gantry parallel robot, a map in x and y plane was applied for the inverse kinematic analysis thus:

Furthermore, the results becomes simple and not trivial as detailed by the following set of principles.

- Everything is done within an inscribed arc
- Cannot go below x – axis
- Cannot go beyond 90º, i.e. above y – axis

Points (11, 8) were arbitrarily picked for the inverse kinematic analysis thus (see figure 4):

The points can reached either by arc down (i.e. coming from the top) or arc upward (i.e. from the bottom), that is, cap downward (clockwise, +ve) or cap upward (anti-clockwise, -ve). This is so, because the answer is always a +ve and –ve values from a quadratic equation.

The analysis continues as follows; (**Note:** multiply x-axis values by 10)

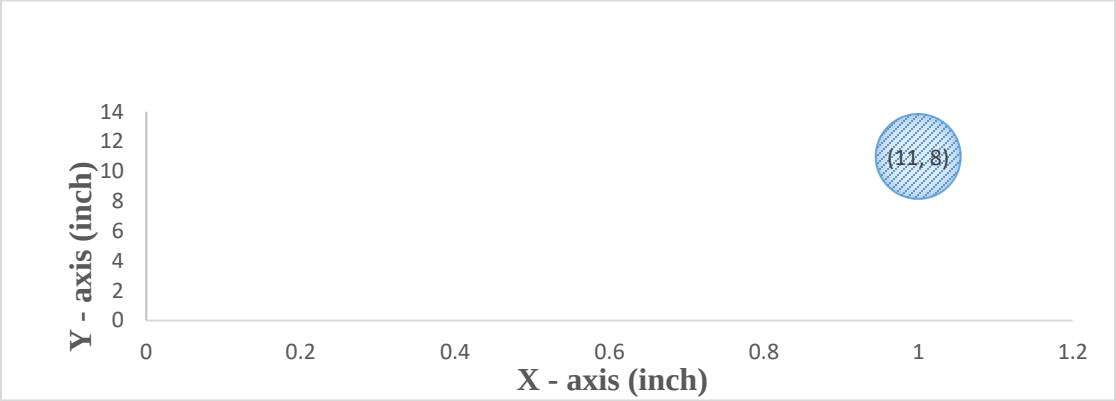

Figure 4: Graph showing the target points for analysis taken arbitrarily

Figure 4 shows the points (11, 8) taken arbitrarily for the inverse kinematic analysis drawn on a plane to determine the length of the kinematic chain from the origin (0, 0), that is, pick up spot to the target spot, that is, point (11, 8).

Furthermore, for the inverse kinematic analysis, the distance from the pick up to the target spot was assumed to have constituted not just a single link, but a number of links forming a kinematic chain thus. Stepper motors were used for this motion actuation.

Table 3: Link Definition

S/N	LINK NAME	DESCRIPTION
1	Shoulder	Base link or the link connected to the origin
2	Elbow	Middle link or the link in between shoulder and wrist
3	Wrist	Target link or the link connected to the end-effector

Let; Wrist length (A) = 5 inch, Elbow length (B) = 5 inch, Shoulder length (C) = 7 inch

Note: decimal figures were avoided, in order to make the analysis simple and not trivial.

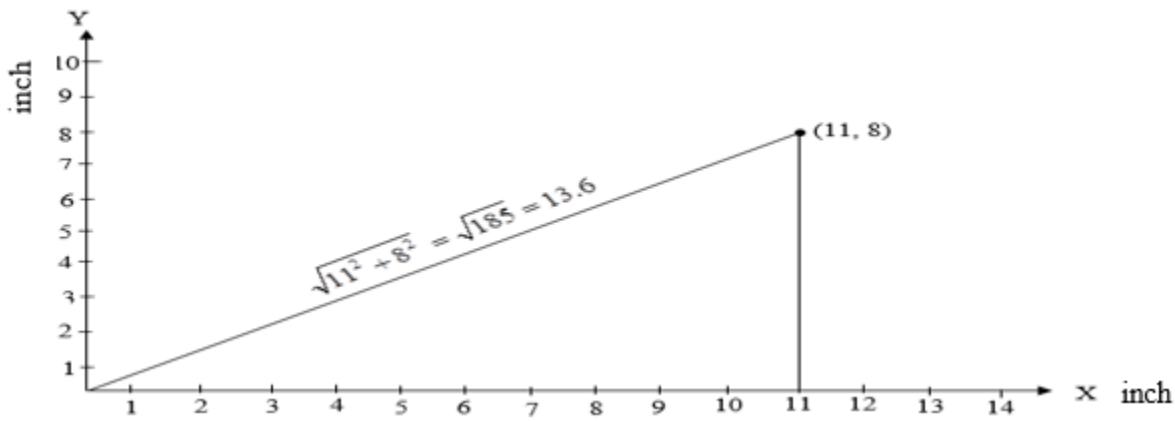

Figure 5: Graph showing length of kinematic chain determined as a hypotenuse

Figure 5 shows the hypotenuse of the plane calculated as the length of the kinematic chain from the pick-up location (origin) to the target location (11, 8).

Origin: (0, 0) x = 0 y = 0 - or - v = 0 w = 0
Target: (11, 8) x = 11 y = 8 - or - h = 11 k = 8
Shoulder: 7 inch (makes a 7 inch radius, origin stepper)
Elbow: 5 inch (makes a 5 inch radius)
Wrist: 5 inch (makes a 5 inch radius, target stepper)

Table 4: Kinematic Analysis/Calculation (calculation of links slope & intersection points)

Initial Data	Calculation / Analysis	Remark
	(i) Calculating slope of the link (arm) as a line: $y = mx + b$ ---------- (7) $m = \frac{Dy}{Dx} = \frac{y_2 - y_1}{x_2 - x_1}$, or $m = \frac{k-w}{h-v}$ ---------- (8) $\Rightarrow m = \frac{8-0}{11-0} = \frac{8}{11}$ ------ (9), Put eqn. (9) in (7) and take x = 11 & y = 8 $8 = (8/11) \times 11 + b$, $\Rightarrow b = 0$ ------ (10), Put (10) in (7) 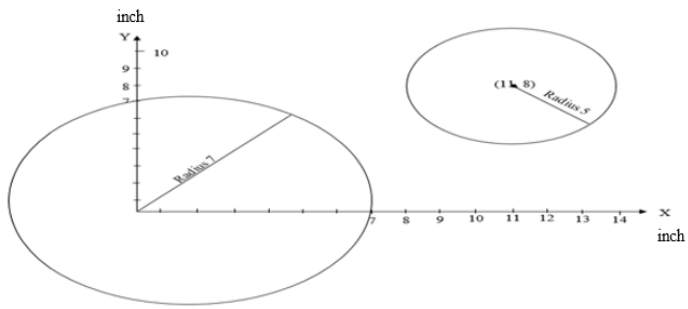 **Figure 6: Graph showing perimeters (ellipse) of the points at which the links were set at**	$y = (8/11)x$ ---------- (11)
Where r = radius, a = h = x – axis coordinate, b = k = coordinate on y - axis Where; a = 1.53, b = -33.64, and c = 160 The coefficients involve fractions, almighty formula was applied thus (equation 17):	**(ii) Calculating the point where the link intersects the perimeter of ellipse of analysis:** $(x-a)^2 + (y-b)^2 = r^2, or\ (x-h)^2 + (y-k)^2 = r^2$ ------ (12) $\Rightarrow (x-11)^2 + (y-8)^2 = 25$ $x^2 - 22x + 121 = 25$ ----- (13), $y^2 - 16y + 64 = 25$ ------ (14) Substitute slope for y, i.e. put eqn. (11) in (14) $\Rightarrow ((8/11)x)^2 - 16((8/11)x) + 64 = 25$ $\frac{64}{121}x^2 - \frac{128}{11}x + 64 = 25$ ---- (15), Combine eqn. (13)&(15) $1.53x^2 - 33.64x + 160 = 0$ ---------- (16) $x = \frac{-b \pm \sqrt{b^2 - 4ac}}{2a}$ ---------- (17) $\Rightarrow x = \frac{33.64 \pm \sqrt{1131.65 - 979.2}}{3.06} = \frac{33.64 \pm 12.35}{3.06}$ $x = 15.03$ -or- 6.96 Put eqn. (18) in (11); i.e. slope eqn. $\Rightarrow y = (8/11)x = (8/11) \times 6.96$	$\therefore x = 6.96$ (taking smaller value) ------ (18) $y = 5.06$ -- (19)

	(1) Points where the slope crosses the circle are (6.96, 5.06) **(2)** Pythagorean theorem was used to calculate the distance from the origin (0, 0) to the new point (6.96, 5.06) $\Rightarrow dist = \sqrt{x^2 + y^2} = \sqrt{(6.96)^2 + (5.06)^2} = 8.61$ ----- (20) 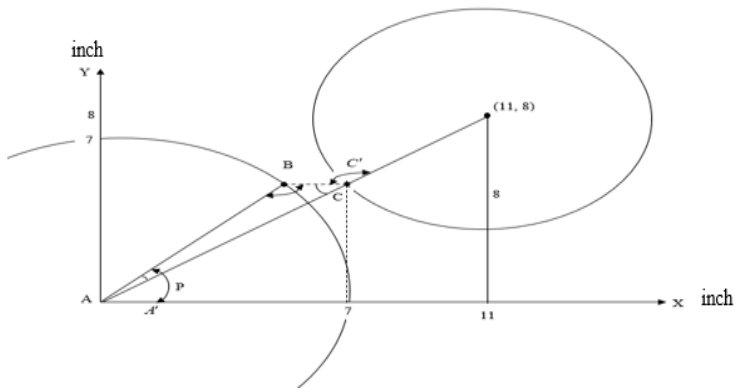 **Figure 7: Graph showing positions & angles at which the links (arm, elbow, and wrist) were set at**	
Let; A = 5mm(length of wrist/ target stepper) B = 8.61mm (length from origin to new point), **eqn. (20)** C = 7mm(length of shoulder/ origin stepper)	Having 3 known sides of a triangle, Side – Side – Side calculation was used to find all 3 angles of the triangle. $A^2 = B^2 + C^2 - 2BC\cos A$ $\cos(A) = (B^2 + C^2 - A^2)/2(B)(C)$ ---------- (21), Similarly; $\cos(B) = (A^2 + C^2 - B^2)/2(A)(C)$ ---------- (22) $\cos(C) = (A^2 + B^2 - C^2)/2(A)(B)$ ---------- (23) $\Rightarrow \cos(A) = (74.13 + 49 - 25)/120.54$, Similarly; $A = \cos^{-1}(0.8141) = 35.50^0$ $\cos(B) = (49 + 25 - 74.13)/70$ $\cos(C) = (25 + 74.13 - 49)/86.1$ Alternatively; $C = (180 - (90.11 + 35.50)) = 54.39^0$ $\tan P = 8/11 = 0.7273$ $\Rightarrow P = \tan^{-1}(0.7273) = 36.03^0$ $A' = A + P = 35.50 + 36.03$ $C' = 180 - C = 180 - 54.39$	$A = 35.50^0$ $B = 90.11^0$ $C = 54.39^0$ $A' = 71.53$ $C' = 125.61^0$

3. Results and discussion

For the kinematics analysis, a number of researchers have proposed, explained and followed scientific methods, to mention a few, the likes of;

Mahir et al. (2015) in the research therein, a gantry robot was analyzed kinematically applying a user interface based on visual basic and MATLAB GUI (Graphical User Interface). The research presented a software kinematics analysis approach.

Abdur Rosyid et al. (2022) presented a reconfigurable parallel robot on-structure machining of large structures. The analysis was carried out and solved numerically using Levenberg-Marquardt algorithm. The research also presented a software kinematics analysis.

Swaminath et al. (2023) carried out a kinematics analysis and obtained results using CAD algorithm. The kinematics analysis was done by mapping tilt and torsion angles for a 3-SPS-U parallel mechanism. Also, this research presented a software kinematics analysis method.

A reseanable number of other researchers have presented analysis on robot kinemtics and at once discussed it but, neither software analysis method nor mathematical model equations and solutions were provided. Example, the likes of; Erik Wernholt (2004), Stig Moberg (2010).

3.1 Forward Kinematic Analysis Results

From table 4, it was shown that as y-axis level was kept constant (1st set up of experiment), there was only a slight change in the angles, and that was due to some little error/deviation in the links displacement. The angular displacement varies but only a little, due to the different positions of pick-up and drop locations. But, the link length increases due to the increase in lengths of the target (drop) locations from the origin along x-axis. This shows that the result really conformed to the desired design intentions, and thus, the results appears to be true. Table 4 shows the correlation thus:

Table 0: Table showing forward kinematic analysis results of the robot (1st set up)

x (mm)	y (mm)	t (s)	θ^o	θ (rad.)	r (mm)	ω (rad/s)
1.09	4.97	20	78	1.36	5.42	0.07
2.04	5.02	20	68	1.19	5.41	0.06
2.99	5.01	20	59	1.03	5.81	0.052
4.03	4.98	20	51	0.89	6.41	0.045
5.13	5.04	20	45	0.97	7.26	0.04

In the second method of experiment (table 5), x and y levels were increased linearly and correspondingly and from that table, the result appears true because the links angles remains almost the same for every pre-defined pick-up and drop locations. There was an increase in the length of the links and that is because of the increase in x and y levels resulting from the intention of pre-defining different number of pick-up and drop (target) spots consecutively.

Table 5 shows the true correlation of the analysis data and also proven to be true.

Table 5: Table showing forward kinematic analysis results of the robot (2nd set up)

x (mm)	y (mm)	t (s)	θ°	θ (rad.)	r (mm)	ω (rad/s)
1.01	1.04	20	46	0.803	1.45	0.04
1.99	2.03	20	46	0.803	2.82	0.04
3.01	3.02	20	45.1	0.787	4.26	0.039
3.97	4.01	20	45.3	0.791	5.64	0.04
5.01	5.06	20	45.3	0.791	7.12	0.04

The orientation of the end effector and links in terms of the frame positions can be presented applying Denavit-Hartenberg (D-H) method, the result can be expressed as: for table 4 and 5;

$$X_{\omega i} = \begin{bmatrix} r_1 \cos\theta_1 & r_1 \sin\theta_1 & 0 \\ r_2 \cos\theta_2 & r_2 \sin\theta_2 & 0 \\ r_3 \cos\theta_3 & r_3 \sin\theta_3 & 0 \\ r_4 \cos\theta_4 & r_4 \sin\theta_4 & 0 \\ r_5 \cos\theta_5 & r_5 \sin\theta_5 & 0 \end{bmatrix} (x, \quad y, \quad 0)$$

For i = 1,2…5

3.2 Inverse Kinematic Analysis Results

The graph (figure 8) shows the end result of the inverse kinematic analysis thus: Figure 8 shows the new targeted angles and positions where the links (shoulder, elbow, and wrist) were set at from pick-up position (origin) to the drop (target) position.

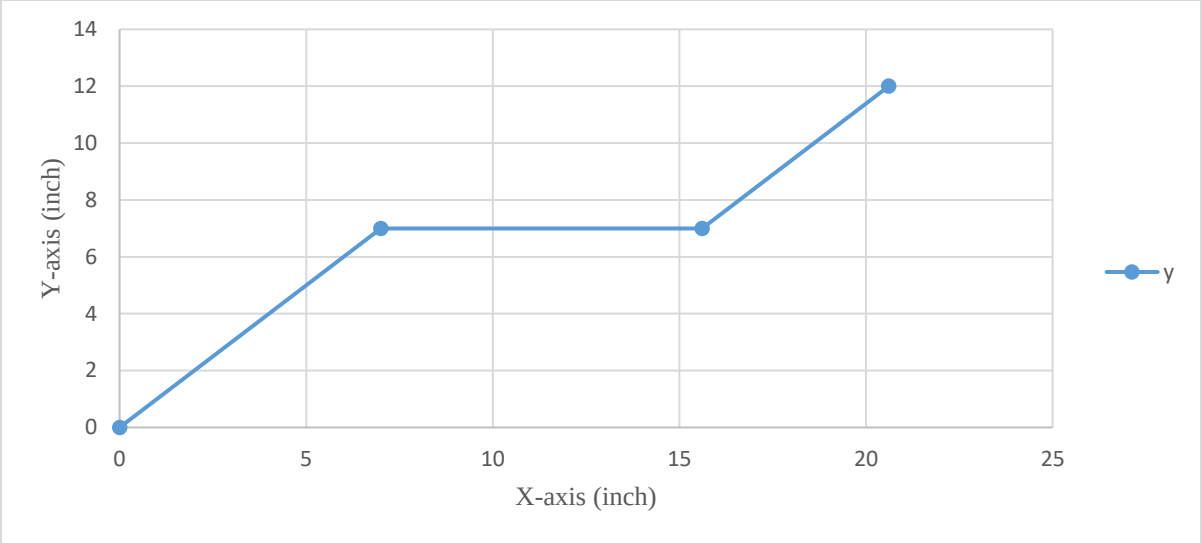

Figure 8: Graph showing the end result of the analysis where the links angles & positions were set at

It is important to note that any fitting errors/deviations come across in the forward and inverse kinematic analyses can be attributed to several factors, including measurement inaccuracies, inherent system noise (internal/external), and mathematical modeling assumptions. The slight deviations in the readings of the links displacements and measured angles are within an acceptable range (±1) considering the complexity of the system and the inherent uncertainties involved.

4. CONCLUSIONS

In this study, a novel gantry-based parallel robot manipulator was analysed kinematically and evaluated for bricklaying applications in the construction industry. The objective was to establish and evaluate the kinematic analysis of the robot manipulator, both forward and inverse kinematic analyses. The gantry-based parallel robot manipulator was successfully analyzed kinematically using appropriate considerations and mathematical modeling procedures, principles, and assumptions. The robot's operational principle and algorithm were carefully defined to ensure the workability/performance integrity of the manipulator. The kinematic modeling of the robot was evaluated applying a 2D planar map test in x – y plane, where different setups were assessed. The results indicated linear relationships and demonstrated the robot's ability to perform bricklaying tasks effectively.

Furthermore, the forward and inverse kinematic analyses were carried out applying geometric, trigonometric, and mechanics of motion approach. The study applied a two-method kinematic analysis procedure for the forward kinematics. The results shows a range of values for the displacements and orientation of the links. Two experimental procedures gave a maximum difference of 0.03rad/s and 0.47rad using the first setup and 0.001rad/s and 0.016rad using the second setup, in the displacement and orientation of the links respectively.

It is important to note that these differences in the measured values of the links displacement and orientation can be attributed to several factors, including measurement inaccuracies, inherent system noise, and mathematical modeling assumptions. The inverse kinematics gave a displacent result of A(5mm), B(8.61mm), and C(7mm) and orientation of $A'(71.53^0)$, $B(90.11^0)$ and $C'(125.61^0)$.The findings of this study contributes to the advancement of robotic systems in the construction industry, offering potential benefits in terms of efficiency, safety, productivity, and kinematics.

Comparing this result with that of Mahir et al. (2015), Abdur Rosyid et al. (2022) and Swaminath et al. (2023), herein, mathematical equations were applied and similar solutions were obtained numerically and not by the application of software analysis.

Also, in comparison with the analysis results of Mahir et al. (2015), herein, the links were assumed to combine together forming a kinematic chain which in turn simplified the analysis further.

Acknowledgements

The authors acknowledge the support offered by Engr. Awwal Isa Bello, Mallam Ibrahim, Mallam Musa Nari, and Ayodeji Nathaniel Oyedeji, as well as the staff and students of the Department of Mechanical Engineering, Ahmadu Bello University, Zaria, Nigeria.

Conflicts of Interests

The authors declare no competing interests

Authors' Contributions

M.H.I. is responsible for data collection, methodology, data analysis, and writing of the original draft. U.A.U. is responsible for the conceptualization, supervision, methodology and review of the original draft. M.A.O. is responsible for the conceptualization, supervision, methodology, and review of the original draft.

References

[1] M. Javaid, A. Haleem, R. P. Singh, and R. Suman, "Substantial capabilities of robotics in enhancing industry 4.0 implementation," *Cognitive Robotics*, vol. 1, pp. 58–75, Jan. 2021, doi: 10.1016/J.COGR.2021.06.001.

[2] S. Luhar and I. Luhar, "Additive Manufacturing in the Geopolymer Construction Technology: A Review," *The Open Construction & Building Technology Journal*, vol. 14, no. 1, pp. 150–161, Aug. 2020, doi: 10.2174/1874836802014010150.

[3] O. Adepoju, "Robotic Construction Technology," *Springer Tracts in Civil Engineering*, pp. 141–169, 2022, doi: 10.1007/978-3-030-85973-2_7/COVER.

[4] T. Bruckmann, H. Mattern, A. Spengler, C. Reichert, A. Malkwitz, and M. König, "Automated Construction of Masonry Buildings using Cable-Driven Parallel Robots".

[5] F. P. Bos *et al.*, "The realities of additively manufactured concrete structures in practice," *Cem Concr Res*, vol. 156, p. 106746, Jun. 2022, doi: 10.1016/J.CEMCONRES.2022.106746.

[6] C. Y. Lai, D. E. Villacis Chavez, and S. Ding, "Transformable parallel-serial manipulator for robotic machining," *International Journal of Advanced Manufacturing Technology*, vol. 97, no. 5–8, pp. 2987–2996, Jul. 2018, doi: 10.1007/S00170-018-2170-Z/METRICS.

[7] C. Yang, W. Ye, and Q. Li, "Review of the performance optimization of parallel manipulators," *Mech Mach Theory*, vol. 170, p. 104725, Apr. 2022, doi: 10.1016/j.mechmachtheory.2022.104725.

[8] R. Simoni, P. R. Rodriguez, P. Cieslak, L. Weihmann, and A. P. Carboni, "Design and kinematic analysis of a 6-DOF foldable/deployable Delta parallel manipulator with spherical wrist for an I-AUV," *OCEANS 2019 - Marseille, OCEANS Marseille 2019*, vol. 2019-June, Jun. 2019, doi: 10.1109/OCEANSE.2019.8867496.

[9] M. O. Afolayan, D. S. Yawas, C. O. Folayan, and S. Y. Aku, "Mechanical Description of a Hyper-Redundant Robot Joint Mechanism Used for a Design of a Biomimetic Robotic Fish," *Journal of Robotics*, vol. 2012, pp. 1–16, 2012, doi: 10.1155/2012/826364.

[10] Z. A. Karam and M. A. Neamah, "Design, Implementation, Interfacing and Control of Internet of Robot Things for Assisting Robot," *International Journal of Computing and Digital Systems*, vol. 11, no. 1, pp. 387–399, 2022, doi: 10.12785/IJCDS/110132.

[11] B. K. Panda, S. S. Panigrahi, G. Mishra, and V. Kumar, "Robotics for general material handling machines in food plants," *Transporting Operations of Food Materials within Food Factories: Unit Operations and Processing Equipment in the Food Industry*, pp. 341–372, Jan. 2023, doi: 10.1016/B978-0-12-818585-8.00005-2.

[12] J. Gunnar, "Dynamical Analysis and System Identification of the Gantry-Tau Parallel Manipulator," 2005, Accessed: May 13, 2023. [Online]. Available: https://urn.kb.se/resolve?urn=urn:nbn:se:liu:diva-5322

[13] "Robotic gantry with end effector for product lifting," Nov. 2018.

[14] C. Ye, N. Chen, L. Chen, and C. Jiang, "A variable-scale modular 3D printing robot of building interior wall," *Proceedings of 2018 IEEE International Conference on Mechatronics and Automation, ICMA 2018*, pp. 1818–1822, Oct. 2018, doi: 10.1109/ICMA.2018.8484433.

[15] A. N. Oyedeji, U. A. Umar, L. S. Kuburi, A. A. Edet, and Y. Mukhtar, "Development and performance evaluation of an oil palm harvesting robot for the elimination of ergonomic risks associated with oil palm harvesting," *Journal of Agricultural Engineering*, vol. 53, no. 3, Sep. 2022, doi: 10.4081/JAE.2022.1388.

[16] J. Meena, T. K. Sunil Kumar, and T. R. Amal, "Design and Implementation of a Multi-purpose End-effector Tool for Industrial Robot," *2021 International Symposium of Asian Control Association on Intelligent Robotics and Industrial Automation, IRIA 2021*, pp. 70–76, Sep. 2021, doi: 10.1109/IRIA53009.2021.9588746.

[17] K. Mohamed, H. Elgamal, and A. Elsharkawy, "Dynamic analysis with optimum trajectory planning of multiple degree-of-freedom surgical micro-robot," *Alexandria Engineering Journal*, vol. 57, no. 4, pp. 4103–4112, Dec. 2018, doi: 10.1016/J.AEJ.2018.10.011.

[18] E. V. Gaponenko, D. I. Malyshev, and L. Behera, "Approximation of the parallel robot working area using the method of nonuniform covering," *J Phys Conf Ser*, vol. 1333, no. 5, p. 052005, Oct. 2019, doi: 10.1088/1742-6596/1333/5/052005.

[19] A. M. Hoover, E. Steltz, and R. S. Fearing, "RoACH: An autonomous 2.4g crawling hexapod robot," *2008 IEEE/RSJ International Conference on Intelligent Robots and Systems, IROS*, pp. 26–33, 2008, doi: 10.1109/IROS.2008.4651149.

[20] R. V. Martinez *et al.*, "Robotic Tentacles with Three-Dimensional Mobility Based on Flexible Elastomers," *Advanced Materials*, vol. 25, no. 2, pp. 205–212, Jan. 2013, doi: 10.1002/ADMA.201203002.

[21] Z. Zou *et al.*, "Real-time Full-stack Traffic Scene Perception for Autonomous Driving with Roadside Cameras," *Proc IEEE Int Conf Robot Autom*, pp. 890–896, 2022, doi: 10.1109/ICRA46639.2022.9812137.

[22] H. A. Sonar, J.-L. Huang, and J. Paik, "Soft Touch using Soft Pneumatic Actuator–Skin as a Wearable Haptic Feedback Device," *Advanced Intelligent Systems*, vol. 3, no. 3, p. 2000168, Mar. 2021, doi: 10.1002/AISY.202000168.

[23] L. Ljung, "System Identification," pp. 163–173, 1998, doi: 10.1007/978-1-4612-1768-8_11.

[24] M. Hofer and R. D'Andrea, "Design, Modeling and Control of a Soft Robotic Arm," *IEEE International Conference on Intelligent Robots and Systems*, pp. 1456–1463, Dec. 2018, doi: 10.1109/IROS.2018.8594221.

[25] S. Gale, H. Rahmati, J. T. Gravdahl, and H. Martens, "Improvement of a Robotic Manipulator Model Based on Multivariate Residual Modeling," *Front Robot AI*, vol. 4, p. 28, Jul. 2017, doi: 10.3389/FROBT.2017.00028/BIBTEX.

[26] B. Alkali "Design and Development of Parallel and Serial Robot Manipulators for Bottle Capping Process" 2014. A Ph.D. Thesis, Department of Mechanical Engineering, Ahmadu Bello University, Zaria.

[27] M. W. Spong, Vidyasagar and M. Wiley. Robot Dynamics and Control. Prentice-Hall Int., London, 1989.

[28] L. Sciavicco and B. Siciliano. Modeling and Control of Robotic Manipulators. The Math Works Inc., Sherborn, MA, USA, Springer, 2000.

[29] A. C. Mark. Obstacle avoidance in Multi-Robotic System. Robots and Autonomous. Canada: 3rd Edition, John Wiley and Sons Inc, 1998.

[30] G. D. Nicholas & A. Edward (2009). Kinematic Modeling of six Degree of Freedom Tri-stage Micro-Positioned. Proceedings of the American Society of Precision Engineering, 16th Annual Meeting, (pp. 200-203).

[31] Z. G. Woldu. Design and Control of a Five bar Linkage Parallel Manipulator with Flexible Arms. Milan, Spain: An M.Sc. Thesis, Polytechnic Di Milano, Spain, 2010.

[32] M. Donya, Y. Aghil, B. Shanaz, & M. Hessam (2008). Design Fabrication and Hydrodynamic Analysis of a Biomimetic Robot Fish (Vol. 4). International Journal of Mechanics.

[33] H. I. Musa, U. A. Umar, M. O. Afolayan, and O. N. Ayodeji (2023). Development and Performance Evaluation of a Bricklaying gantry-Based Parallel Robot Manipulator. *Journal of Engineering, Science and Computing (JESC). The Islamic University Journal of Applied Sciences Volume V, Issue I*, jesc.iu.edu.sa/Main/Article/112, pp. 71 – 90, July 2023.

[34] A. I. I. Mahir and M. K. Mohammed (2015). Gantry Robot Kinematic Analysis User Interface Based on Visual Basic and MATLAB.*International Journal of Science and Research (IJSR).* ISSN (online): 2319-7064. Mechanical Engineering Department, Tianjin Univerity of Technology and Education, Tianjin 300222, China.

[35] A. Rosyid, C. Steanini and B. El-Khasawneh (2022). A Reconfigurable Parallel Robot for On-Structure Machining of Large Structures. *Robotics 2022, 11, 110. https:/ /doi.org/10.3390/robotics11050110.* https:/ /www.mdpi.com/journal/robotics.

[36] V. Swaminath and D. Chablat (2023). Mapping the Tilt and Torsion Angles for a 3-SPS-U Parallel Mechanism. *Robotics 2023, 12, 50. https:/ /doi.org/10.3390/robotics12020050.* https:/ /www.mdpi.com/journal/robotics.